Statistical and Nonstatistical Dynamics in the Unimolecular Decomposition of Vinyl Bromide

Ronald D. Kay*

Department of Chemistry, Gordon College, 255 Grapevine Road, Wenham, Massachusetts 01984

Lionel M. Raff

Department of Chemistry, Oklahoma State University, Stillwater, Oklahoma 74078

Received: August 23, 1996; In Final Form: November 14, 1996[⊗]

Rate constants have been computed for three unimolecular decomposition reactions of vinyl bromide for several energies in the range 5.23−7.67 eV, using statistical variational efficient microcanonical sampling−transition-state theory (EMS-TST) on a global vinyl bromide potential energy surface. The EMS-TST results are compared with those obtained from a previously reported classical trajectory study on the same potential energy surface [*J. Phys. Chem.* **1995**, *99*, 2959] in order to assess the extent to which vinyl bromide unimolecular decomposition is governed by statistical dynamics. For the three-center HBr elimination reaction, it is found that $k_{EMS-TST}$ is greater than $k_{trajectory}$ by a factor of 1.5−3.5 over the energy range considered. For the C−Br bond scission, the EMS-TST and trajectory results at lower energies are equal within the statistical error in the trajectory calculations, while at higher energies $k_{EMS-TST}$ exceeds $k_{trajectory}$ by a factor of 1.4−2.9. The EMS-TST calculations also reproduce a surprising result from the trajectory study, that the rate constant for three-center HBr elimination is an order of magnitude greater than that for C−Br bond scission throughout the energy range, even though the barrier height for the latter reaction is 0.34 eV lower. These results imply that three-center HBr elimination and C−Br bond scission are governed by statistical dynamics. For the three-center H_2 elimination reaction, however, $k_{trajectory}$ is greater than $k_{EMS-TST}$ by a factor of 2−4 at lower energies and a factor of 5−7 at higher energies. This result necessarily implies that the dynamics of the three-center H_2 elimination are nonstatistical. The nonstatistical behavior for this reaction is attributed to a breakdown in the coupling among vibrational modes as the H_2 fragment departs, which leaves energy in excess of the statistically predicted amount in the dissociation coordinate. A study of intramolecular vibrational relaxation (IVR) rates and pathways in vinyl bromide [*J. Phys. Chem.* **1996**, *100*, 8085] supports this conclusion. The IVR analysis also shows that such a breakdown in mode-to-mode coupling does not exist for the three-center HBr elimination and that nearly global randomization of the internal energy rapidly occurs as the system moves through the transition-state region for HBr elimination. Thus, the nature of IVR on the vinyl bromide potential surface used in this work is consistent with the present EMS-TST results showing that three-center HBr elimination is well-described by statistical reaction rate theory, while three-center H_2 elimination is not.

I. Introduction

It is generally established that small, three- or four-atom molecules, or single-center molecules such as CH_4, generally obey the central assumption of all statistical theories that internal energy is randomly distributed over phase space so that all phase-space points of energy E are sampled with equal probability.[1] Recent examples have been provided by Peslherbe and Hase,[2] who studied the decomposition dynamics of Al_3 and found excellent agreement between statistical theory and trajectories. Klippenstein and Koess[3] have obtained similar agreement between statistical theory and *ab initio* scattering results for the $He + H_2^+ \rightarrow HeH^+ + H$ reaction. Klippenstein and Radivoyevitch[4] found statistical behavior in their investigation of NO_2 dissociation. Recent results reported by Hu and Hase[5] have verified that the decomposition of CH_4 is a statistical process. The agreement between experiment and variational transition-state theory calculations for the reaction of OH radicals with CH_4 reported by Truong and Truhlar[6] and Melissas and Truhlar[7] indicates the statistical nature of this system. Similar results for the $CH_3 + H_2$ and the $OH + H_2$ reactions have been obtained by Gonzalez-Lafont *et al.*[8]

When the reacting system is polyatomic, however, the existence of internal modes essentially decoupled from the reaction coordinate increases the probability that intramolecular vibrational relaxation (IVR) bottlenecks will exist. Consequently, more and more such systems are being found that do not behave in accordance with statistical theory. For example, experimental investigations of the decomposition reactions of substituted benzenes reported by Bersohn and co-workers[9,10] have shown that extensions of RRKM theory are insufficient to explain the translational energy distributions of product hydrogen atoms. Holland and Rosenfeld[11] obtained similar results in the photolysis of $W(CO)_6$. It was found that microcanonical phase-space theory[12,13] could not predict the observed energy disposal patterns. Viggiano *et al.*[14] and Graul and Bowers[15] have investigated the halogen exchange reaction between Cl^- and CH_3Br and found that the measured rate coefficient is independent of the vibration/rotation temperature, which is inconsistent with the predictions of RRKM theory. The CH_3Cl product is also found to have a nonstatistical distribution of internal energy. Van Orden *et al.*[16] obtained a similar result for the exchange reaction between F^- and CH_3Cl. Cho *et al.*[17,18] and Vande Linde and Hase[19] have found the reaction between Cl^- and CH_3Cl to involve nonstatistical behavior with extensive

[⊗] Abstract published in *Advance ACS Abstracts,* January 1, 1997.

S1089-5639(96)02624-2 CCC: $14.00

barrier recrossings and intramolecular dynamics that are not in accord with transition-state assumptions. Carpenter and co-workers[20−24] have found striking nonstatistical branching ratios in several systems whose reaction mechanisms involve large, biradical species.

By comparing the results of trajectory calculations with classical EMS-TST (efficient microcanonical sampling−transition-state theory) and EJS-TST (efficient *J*-conserving sampling−transition-state theory) calculations[25−30] on the same potential energy surfaces, we have identified the presence of nonstatistical dynamics in decomposition reactions of Si_2H_6, 1,2-difluoroethane, and vinyl bromide.[25−29,31−33] In contrast, our previous studies show statistical behavior for SiH_2, the 2-chloroethyl radical,[25−29] and the inversion reactions for bicyclo[2.1.0]-pentane.[34] These results have led us to conclude that *nonstatistical dynamics will be favored whenever motion along the reaction coordinate does not produce large energetic changes in one or more bonds in the remainder of the molecule.* When such energetic changes occur, there will frequently be an enhanced coupling between the dissociation coordinate and the remainder of the molecule that leads to increased IVR rates and decreased reaction rates, both of which will tend to eliminate nonstatistical effects. A second principle postulated by Carpenter and co-workers[20−22] is that *nonstatistical behavior will become more prevalent as the energy of the reacting system approaches threshold.* Our results[25−29,31] support this hypothesis.

We have recently examined the dynamics of intramolecular energy transfer in vinyl bromide[33] using the projection method.[35] The calculated total energy decay rates and the pathways of energy flow for initial excitation of each of the 12 vibrational modes in the equilibrium configuration show that the minimum energy decay rate among the 12 modes is at least 3.1 times larger than the trajectory-computed[32] decomposition rate of vinyl bromide with 6.44 eV of excitation energy present. However, it is also found that energy transfer is not globally rapid.[33] In configurations near the minimum energy structure on the optimum dividing surface for three-center H_2 elimination, the intramolecular energy transfer rate for some mode-to-mode processes is slower than the unimolecular dissociation rate. In contrast, energy transfer in configurations near the minimum energy structure on the optimum dividing surface for three-center HBr elimination is globally rapid relative to the HBr elimination rate for all modes except the C−C−Br bend. The energy transfer dynamics for vinyl bromide therefore suggest[33] that three-center HBr elimination may be accurately described by statistical theories, but the corresponding three-center H_2 elimination reaction will probably behave nonstatistically.

In this paper, we report the results of efficient microcanonical sampling−transition state theory (EMS-TST) calculations[25−29] of the reaction rates for three-center elimination of HBr, C−Br bond scission, and three-center elimination of H_2 on the same potential hypersurface used in previous trajectory studies of these processes.[32] We have previously noted[26−29] that if $k_{\mathrm{EMS-TST}}$ is less than $k_{\mathrm{trajectory}}$ on the same potential energy surface, the system must behave nonstatistically. Thus, by comparing the results of the present EMS-TST calculations with the trajectory results, we can assess the extent to which vinyl bromide unimolecular decomposition is governed by statistical dynamics. The remainder of the paper is organized as follows: section II provides a brief general description of the EMS-TST procedure and describes the details of its implementation here for vinyl bromide unimolecular decomposition; section III presents and discusses the comparison between the EMS-TST and trajectory results; and section IV summarizes our conclusions.

II. Computational Procedures

According to classical transition-state theory (TST), the microcanonical rate constant, $k(E)$, for a unimolecular reaction is given by[36]

$$k(E) = \frac{1}{2}\frac{\int \mathrm{d}\Gamma\ \delta[H(\Gamma) - E]\ \delta(q_{\mathrm{RC}} - q_{\mathrm{C}})|\dot{q}_{\mathrm{RC}}|}{\int \mathrm{d}\Gamma\ \delta[H(\Gamma) - E]} \tag{1}$$

where Γ is the set of phase-space coordinates and momenta $\{\mathbf{q},\mathbf{p}\}$, $H(\Gamma)$ is the Hamiltonian of the system, E is the total energy, $q_{\mathrm{RC}} = q_{\mathrm{RC}}(\mathbf{q})$ is the reaction coordinate, q_{C} is the critical value of q_{RC}, i.e., the location of the transition-state dividing surface separating reactants from products, $\dot{q}_{\mathrm{RC}} = \dot{q}_{\mathrm{RC}}(\mathbf{q})$ is the velocity along the reaction coordinate, and the integrals in the numerator and denominator are understood to be over the phase space of the reactants only. While eq 1 can be evaluated directly using Metropolis sampling[37] over reactant phase space,[36,38] it can also be transformed into an expression amenable to evaluation by Metropolis sampling over the reactant configuration space only, provided that the Hamiltonian is separable, that is,

$$H(\Gamma) = T(\mathbf{p}) + V(\mathbf{q}) \tag{2}$$

where T is the kinetic energy and V is the potential energy. Substitution of eq 2 into eq 1 has been shown[26,39] to give for $k(E)$ the expression

$$k(E) = \frac{1}{2}\frac{\int \mathrm{d}\mathbf{q}\ W(\mathbf{q})\ \delta(q_{\mathrm{RC}} - q_{\mathrm{C}})\langle|\dot{q}_{\mathrm{RC}}|\rangle}{\int \mathrm{d}\mathbf{q}\ W(\mathbf{q})} \tag{3}$$

in which $W(\mathbf{q})$ is the efficient microcanonical sampling (EMS) weight factor,[40]

$$W(\mathbf{q}) = [E - V(\mathbf{q})]^{(3N-5)/2} \tag{4}$$

and $\langle|\dot{q}_{\mathrm{RC}}|\rangle$ is the momentum-averaged absolute velocity along the reaction coordinate, given by

$$\langle|\dot{q}_{\mathrm{RC}}|\rangle = \frac{\int \mathrm{d}\mathbf{p}\ \delta[T(\mathbf{p}) - K]|\dot{q}_{\mathrm{RC}}|}{\int \mathrm{d}\mathbf{p}\ \delta[T(\mathbf{p}) - K]} \tag{5}$$

where $K \equiv E - V(\mathbf{q})$ is the kinetic energy at configuration $\mathbf{q}$. Equation 3 can be evaluated by a Markov walk over reactant configuration space, with momenta being required only for the evaluation of the average absolute velocity when the walk reaches a configuration at the transition state. Use of eqs 3−5 to evaluate microcanonical unimolecular rate constants is called the EMS-TST method[26] and is the method used in this work to evaluate $k(E)$ for various unimolecular decomposition reactions of vinyl bromide. The potential energy surface, $V(\mathbf{q})$, employed in the calculations is our previously published[32] global potential for vinyl bromide.

The EMS weight factor $W(\mathbf{q})$ used in the Markov walk gives a larger weight to configurations of lower potential energy, which means that configurations in the transition-state region are sampled much less frequently than those near the equilibrium configuration. Thus, evaluation of the integral over the transition-state region in the numerator of eq 3 for $k(E)$ will converge relatively slowly. However, the convergence rate can be increased by introducing importance sampling into the Markov walk.[26] To do this, an importance sampling function $I(\mathbf{q})$,

given by

$$I(\mathbf{q}) = [E - V(\mathbf{q})]^{\alpha} \tag{6}$$

where α is an adjustable parameter, is inserted into eq 3 to give

$$k(E) = \frac{1}{2}\frac{\int \mathrm{d}\mathbf{q}\, W_{\mathrm{eff}}(\mathbf{q})\, I(\mathbf{q})\, \delta(q_{\mathrm{RC}} - q_{\mathrm{C}})\, \langle|\dot{q}_{\mathrm{RC}}|\rangle}{\int \mathrm{d}\mathbf{q}\, W_{\mathrm{eff}}(\mathbf{q})\, I(\mathbf{q})} \tag{7}$$

in which the effective weight factor $W_{\mathrm{eff}}(\mathbf{q})$ is

$$W_{\mathrm{eff}}(\mathbf{q}) = [E - V(\mathbf{q})]^{(3N-5)/2-\alpha} \tag{8}$$

Increasing the value of α increases the relative weight of configurations of higher potential energy, so that the transition-state region is sampled more frequently and the numerator integral converges more rapidly. On the other hand, the value of the integral in the denominator of eq 3, which covers the whole reactant configuration space, is determined primarily by contributions from regions of low potential energy. If α is increased too much, these regions will be sampled infrequently enough to decrease the convergence rate of the denominator integral. In previous work,[26] choosing α to give the exponent in eq 8 a value between 1 and 1.5 produced good convergence of both numerator and denominator. Thus, in this work the value of α was chosen to be 5.0, which for vinyl bromide (N = 6 atoms) makes the exponent in eq 8 equal to 1.5.

In evaluating eq 7 to find $k(E)$, the average absolute velocity across the transition-state dividing surface, $\langle|\dot{q}_{\mathrm{RC}}|\rangle$, must be evaluated whenever the Markov walk reaches a configuration inside the transition-state region. This can be done for any arbitrary dividing surface using eq 5, which must be evaluated via a Monte Carlo procedure. However, for the special case of simple bond scissions, such as the C−Br bond scission in vinyl bromide, for which the reaction coordinate q_{RC} is the length of the dissociating bond and the dividing surface is thus a sphere of radius equal to q_{C}, eq 5 has been evaluated analytically[25] to give the simple formula

$$\langle|\dot{q}_{\mathrm{RC}}|\rangle = \left(\frac{2K}{\pi\mu}\right)^{1/2}\frac{[(3N-5)/2]!}{[(3N-4)/2]!} \tag{9}$$

where μ is the reduced mass for motion along the reaction coordinate. Furthermore, it has been shown[41] that the same formula also applies to more complicated reactions, as long as the dividing surfaces are spherical and the reduced mass is chosen correctly. For example, in the three-center eliminations of HBr and H_2 from vinyl bromide, eq 9 can be used if q_{RC} is chosen to be the distance between the carbon atom and the HBr or H_2 center of mass, and the reduced mass is obtained using the mass of the carbon atom and the total mass of the HBr or H_2 fragment. In all the calculations reported here, eq 9 has been used to obtain values of $\langle|\dot{q}_{\mathrm{RC}}|\rangle$.

The actual numerical evaluation of eq 7 to get the rate constant $k(E)$ consists of generating a set of M configurations $\{\mathbf{q}_i,\ i = 1, ..., M\}$ via Metropolis sampling with weight W_{eff} (from eq 8) and then using these configurations to compute the Monte Carlo approximant to eq 7, which is

$$k(E) = \frac{1}{2\Delta}\frac{\sum_{i=1}^{M} I(\mathbf{q}_i)\, \Theta(\mathbf{q}_i)\, \langle|\dot{q}_{\mathrm{RC}}|\rangle}{\sum_{i=1}^{M} I(\mathbf{q}_i)} \tag{10}$$

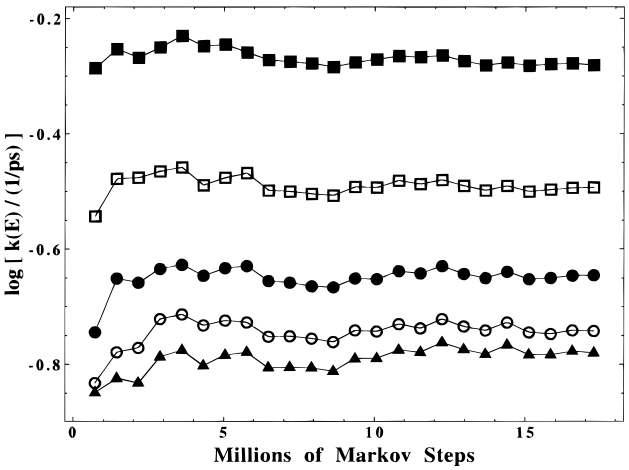

Figure 1. Convergence of the microcanonical rate constant $k(E)$ at several prospective transition-state dividing surfaces for the three-center HBr elimination in vinyl bromide, as a function of Markov walk length at E = 5.23 eV: filled squares (■), q_{C} = 2.4 Å; open squares (□), q_{C} = 2.5 Å; filled circles (●), q_{C} = 2.6 Å; open circles (○): q_{C} = 2.7 Å; filled triangles (▲): q_{C} = 2.8 Å. Lines connecting data points are for visual clarity only.

In eq 10, the delta function $\delta(q_{\mathrm{RC}} - q_{\mathrm{C}})$ from eq 7 is approximated by the simple prelimit form $\Theta(\mathbf{q}_i)/\Delta$, where Δ is the width of the transition-state region and

$$\Theta(\mathbf{q}_i) = \begin{cases} 1, & q_{\mathrm{C}} - \Delta \le q_{\mathrm{RC}} < q_{\mathrm{C}} \\ 0, & \text{otherwise} \end{cases} \tag{11}$$

The Metropolis sampling procedure to generate the set of configurations $\{\mathbf{q}_i\}$ is as follows. An initial configuration $\mathbf{q}_0$ is chosen (see below), and its weight $W_{\mathrm{eff}}(\mathbf{q}_0)$ computed. Then a trial configuration $\mathbf{q}_{\mathrm{trial}}$ is generated from $\mathbf{q}_0$ by moving all three Cartesian coordinates of one or more atoms from their current values by a random amount $(\xi - 0.5)\,\Delta q$, where ξ is a uniform random number between 0 and 1, and Δq is the Markov step size. The trial configuration is first checked to see whether it has crossed any "reflecting surfaces" set up to keep the Markov walk on the energy shell and in reactant configuration space (see below). If so, the trial is discarded and a new one generated by moving the same coordinates using different random numbers. Once a permissible $\mathbf{q}_{\mathrm{trial}}$ has been obtained, its weight $W_{\mathrm{eff}}(\mathbf{q}_{\mathrm{trial}})$ is then computed and compared with $W_{\mathrm{eff}}(\mathbf{q}_0)$. If the ratio $W_{\mathrm{eff}}(\mathbf{q}_{\mathrm{trial}})/W_{\mathrm{eff}}(\mathbf{q}_0)$ is greater than ξ', where ξ' is another uniform random number, then the trial configuration is accepted and becomes $\mathbf{q}_1$, the first configuration in the set $\{\mathbf{q}_i\}$ used to evaluate eq 10. If the ratio $W_{\mathrm{eff}}(\mathbf{q}_{\mathrm{trial}})/W_{\mathrm{eff}}(\mathbf{q}_0)$ is less than ξ', then the trial configuration is rejected, and $\mathbf{q}_0$ becomes $\mathbf{q}_1$. This set of operations constitutes the first "step" of the Markov walk in the Metropolis sampling procedure. The succeeding steps in the Markov walk obtain configuration $\mathbf{q}_{i+1}$ in the set from configuration $\mathbf{q}_i$ using the same set of operations, with new random numbers in each step. After each new step in the walk is taken, the sums in the numerator and denominator of eq 10 are updated. In this work, three of the six vinyl bromide atoms were moved in each Markov step, and the Markov step size was Δq = 0.2 Å. The value of M, the number of configurations used to evaluate $k(E)$ in eq 10, was 18 million. This number of configurations was more than sufficient to ensure convergence of the sums in eq 10, as illustrated by Figure 1, which shows intermediate values of $\log(k)$ at several prospective transition-state dividing surfaces for the three-center HBr elimination reaction, computed at intervals of 720 000 Markov steps in a Markov walk at E = 5.23 eV.

As mentioned above, an initial configuration $\mathbf{q}_0$ must be generated as a starting point for the Markov walk used to

TABLE 1: Reaction Coordinate Definitions and Reflecting Surface Locations Used in the EMS-TST Calculations; Superscripts on Atomic Symbols Refer to the Atom Numbers Defined Below; the Bond Distances r_i and Bond Angles a_j to Which the Table Refers Are Also Defined Below

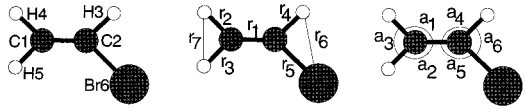

reaction	definition of reaction coordinate	location of dividing surfaces
three-center HBr elimination	distance between C^2 and the H^3Br center of mass, when the H^3-Br distance r_6, is less than 2.0 Å	maximum bond distances: 5 Å for r_1, r_2, r_3, $r_4{}^a$, $r_5{}^a$ minimum bond angles: 90° for a_3; 105° for a_1, a_2, a_4, a_5
C−Br bond scission	C^2-Br distance, r_5	maximum bond distances: 5 Å for r_1, r_2, r_3, r_4 minimum bond angles: 90° for a_3, a_6; 105° for a_1, a_2, a_4, a_5
three-center H_2 elimination	distance between C^1 and the H^4H^5 center of mass, when the H^4-H^5 distance r_7, is less than 1.3 Å	maximum bond distances: 5 Å for r_1, $r_2{}^b$, $r_3{}^b$, r_4, r_5 minimum bond angles: 90° for a_1, a_2, a_6; 105° for a_4, a_5

[a] r_4 and r_5 are subject to this constraint only for configurations in which the H^3Br distance, r_6, is greater than 2.0 Å. [b] r_2 and r_3 are subject to this constraint only for configurations in which the H^4H^5 distance, r_7, is greater than 1.3 Å.

evaluate eq 10. This initial configuration is produced by placing the vinyl bromide molecule in its equilibrium configuration and then doing a "warm-up" Markov walk to reach the configuration $\mathbf{q}_0$, using the procedure outlined above. The purpose of this procedure is to ensure that $\mathbf{q}_0$ is a random configuration characteristic of the total energy E. In this work, the value of M_{warm}, the number of configurations in a warm-up Markov walk, was 100 000. This value of M_{warm} was chosen based on previous work involving disilane, Si_2H_6.[26]

As mentioned earlier, the integrals in eqs 3 and 7 are assumed to be over the reactant configuration space only. In practice, this condition is enforced by restricting the Markov walk in eq 10 to reactant configurations through the use of "reflecting surfaces" at the periphery of reactant configuration space. A reflecting surface would be crossed by the Markov walk if a Markov step produced a configuration $\mathbf{q}$ that (i) was off the energy shell [i.e., $V(\mathbf{q}) > E$], (ii) was past the transition-state dividing surface [i.e., $q_{\text{RC}}(\mathbf{q}) > q_{\text{C}}$], or (iii) caused a particular bond length to exceed some maximum value or a particular bond angle to fall below some minimum value. In this last case, maximum values on bond distances eliminate competing bond scission reactions, while minimum values on bond angles eliminate competing three- and four-center elimination reactions. The values of the maximum bond distances and minimum bond angles used for each of the three dissociation reactions studied here are given in Table 1.

Since the rate constant $k(E)$ computed statistically using eq 3 is an upper bound to the "true" rate constant computed by classical trajectories on the potential energy surface,[1] the value of $k(E)$ should be minimized with respect to the location of the transition-state dividing surface. This minimization procedure can be done using a single Markov walk having several different dividing surfaces $q_{\text{C},i}$, each with an associated transition-state region of width Δ, in the portion of configuration space where the transition state is supposed to be. If $q_{\text{C},1}$ is the location of the innermost dividing surface and there are n_{ts} surfaces separated by a distance δq_{C}, then the positions of the dividing surfaces are given by $q_{\text{C},i} = q_{\text{C},1} + (i - 1)\,\delta q_{\text{C}}$, with $i = 1, ..., n_{\text{ts}}$. When the Markov walk reaches a configuration $\mathbf{q}$ for which $q_{\text{C},j-1} \le q_{\text{RC}}(\mathbf{q}) < q_{\text{C},j}$, then the sums in the numerator and denominator of eq 10 are updated only for the dividing surfaces $q_{\text{C},j}$ through $q_{\text{C},n_{\text{ts}}}$. The sums for the surfaces $q_{\text{C},1}$ through $q_{\text{C},j-1}$ are not updated, since for these surfaces the configuration $\mathbf{q}$ is outside reactant configuration space. When several dividing surfaces are used in this manner, only the outermost surface $q_{\text{C},n_{\text{ts}}}$ is also a reflecting surface for the Markov walk. In this work, for all three of the reactions studied the number of dividing surfaces was $n_{\text{ts}} = 31$ and their spacing was $\delta q_{\text{C}} = 0.1$ Å. For the three-center HBr elimination and the C−Br bond scission reactions, the innermost surface was located at $q_{\text{C},1} = 2.0$ Å, while for the three-center H_2 elimination the innermost surface was at $q_{\text{C},1} = 1.0$ Å.

For each of the three reactions investigated here, the reaction coordinate q_{RC} was assumed to be the distance between the center of mass of the dissociating fragment (HBr for three-center HBr elimination, Br for C−Br bond scission, and H_2 for three-center H_2 elimination) and the carbon atom to which the fragment was bonded in the original vinyl bromide molecule. Also, the reduced mass for motion along the reaction coordinate was computed using the total mass of the dissociating fragment and the mass of the carbon atom. These choices allow the use of eq 9 to compute the average absolute velocity along the reaction coordinate, as mentioned previously. However, using this reaction coordinate definition for the HBr and H_2 elimination reactions was problematic in that, in practice, it did not clearly distinguish between the desired elimination reaction and the competing C−Br or C−H bond scissions. This problem was most acute for the HBr elimination since the center of mass of the HBr fragment lies so close to the Br atom. To fix the problem, a further specification was added to the reaction coordinate definition in the case of the HBr and H_2 eliminations: the H−X separation in the fragment, r_{HX}, was required to be less than some maximum value $r_{\text{HX,max}}$. In this work, $r_{\text{HX,max}}$ was chosen to be 2.0 Å for X = Br and 1.3 Å for X = H. These values were chosen to be somewhat smaller than the H−X separations in the equilibrium geometry of vinyl bromide (2.52 and 1.88 Å, respectively[32]), yet large enough that the potential energies of the HX fragments on the vinyl bromide potential surface[32] at these H−X separations were considerably larger (by more than 0.5 eV) than the average energy in the fragments after reaction.[32] The effectiveness of this method in distinguishing between the three-center HBr elimination and the C−Br bond scission is illustrated in Figure 2, which shows for each reaction the minimum potential energy value obtained at each transition-state dividing surface in a Markov walk at $E = 7.23$ eV. The two curves go to their correct limiting values on the potential energy surface (3.45 and 3.1 eV, respectively[32]).

In this study, rate constants were computed using the EMS-TST method for the three-center HBr elimination, C−Br bond scission, and three-center H_2 elimination reactions of vinyl bromide at total energies E of 5.23, 5.73, 6.23, 6.48, 6.73, 6.98, 7.23, and 7.67 eV and compared with rate constants for these reactions computed using classical trajectories.[32] The total energies used represent zero-point energy plus varying amounts

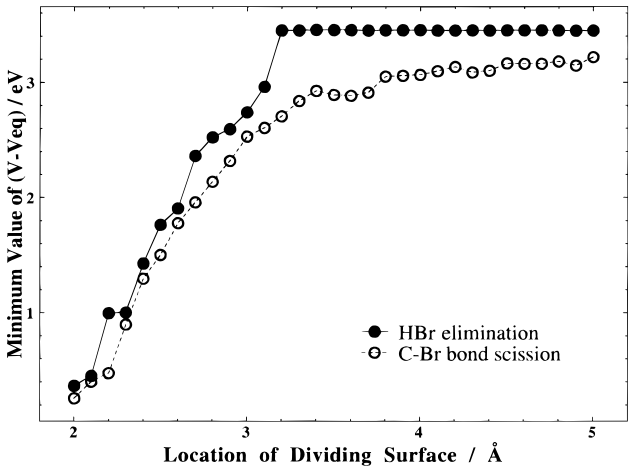

Figure 2. Minimum value of the potential energy V at each transition-state dividing surface for the three-center HBr elimination and for the C−Br bond scission, obtained in each case by a Markov walk at E = 7.23 eV. Ordinate values are plotted with respect to V_{eq}, the global minimum on the vinyl bromide potential energy surface. Lines connecting data points are for visual clarity only.

TABLE 2: Markov Walk Parameters Used in the EMS-TST Calculations

Markov walk parameter	value
number of warm-up Markov steps, M_{warm}	100 000
number of steps in Markov walk, M	18 000 000
number of atoms moved per Markov step	3
Markov step size, Δq/Å	0.2
importance sampling exponent, α	5.0
number of transition-state dividing surfaces, n_{ts}	31
spacing between dividing surfaces, δq_C/Å	0.1
width of each dividing surface, Δ/Å	0.1
location of innermost dividing surface, $q_{C,1}$/Å	2.0[a] or 1.0[b]

[a] For the three-center HBr elimination and C−Br bond scission. [b] For the three-center H_2 elimination.

of excitation energy over the range 4.00−6.44 eV, as in the corresponding trajectory calculations in ref 32. However, the above energies are 0.14 eV greater in each case than the total energies used in the trajectory calculations. The discrepancy comes from the fact that in this work the zero-point energy was taken to be 1.23 eV, which is the Hartree−Fock unscaled harmonic zero-point energy of vinyl bromide reported in ref 32, whereas the trajectory calculations used a zero-point energy of 1.09 eV, which is the value obtained by normal-mode analysis at the vinyl bromide equilibrium geometry on the analytic potential energy surface used here and in ref 32. For each vinyl bromide reaction at each energy, the reported rate constant is the average of six values of the rate constant computed using separate Markov walks with different initial random number seeds. The associated error bar is the 95% confidence limit, given by twice the sample standard deviation of the set of six rate constant values. Table 2 summarizes the values of the Markov walk parameters used in the EMS-TST calculations on vinyl bromide. The trajectory rate constants to which the results of this work were compared are not given explicitly in ref 32. They were found by multiplying the total vinyl bromide decomposition rate constant at each energy (from Figure 7 of ref 32) by the appropriate branching ratio (from Table 18 of ref 32).

In addition to the vinyl bromide calculations described above, a preliminary set of calculations were performed to test the EMS-TST computer program used in this work. In this test, average bond distances and potential energies as well as rate constants for Si−Si bond scission were computed for disilane, Si_2H_6, over the energy range 5.31−9.31 eV and compared with

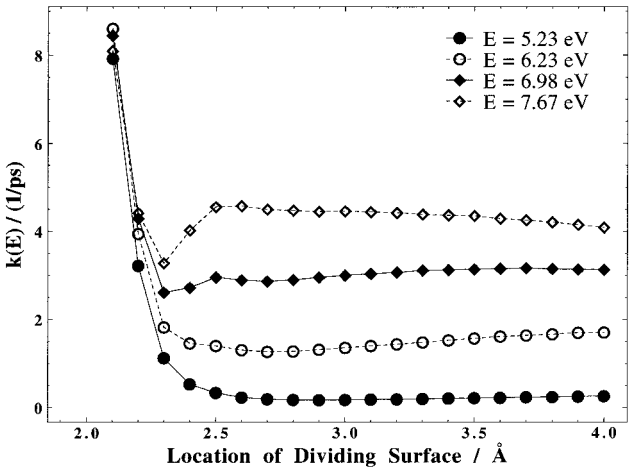

Figure 3. EMS-TST results for k_{HBr}, the microcanonical rate constant for three-center HBr elimination in vinyl bromide, as a function of transition-state dividing surface location, q_C. Results are shown for E = 5.23, 6.23, 6.98, and 7.67 eV. Lines connecting data points are for visual clarity only.

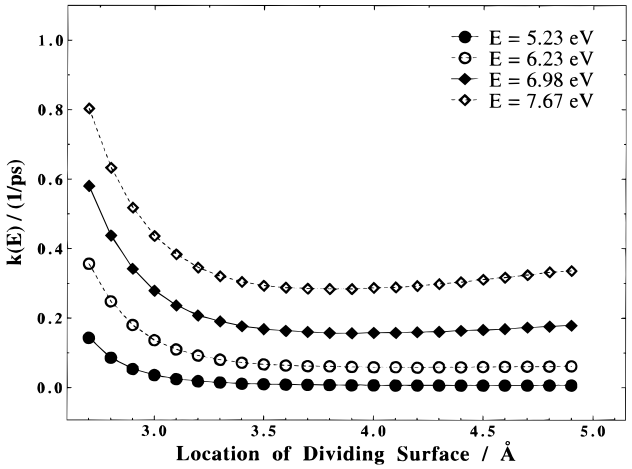

Figure 4. EMS-TST results for k_{C-Br}, the microcanonical rate constant for C−Br bond scission in vinyl bromide, as a function of transition-state dividing surface location, q_C. Results are shown for E = 5.23, 6.23, 6.98, and 7.67 eV. Lines connecting data points are for visual clarity only.

published results for Si_2H_6 using the same potential energy surface.[26] Markov walk parameters for the Si_2H_6 test calculations were identical to those in ref 26. Five Markov walks using different initial random number seeds were used to compute the reported results and their errors at each energy. Our results for average bond distances and potential energies are in excellent agreement with those from ref 26, and the rate constants for Si−Si bond scission generally agree within the statistical error of the calculations.

III. Results and Discussion

The dependence of the EMS-TST value of $k(E)$ on q_C, the location of the transition-state dividing surface, is shown in Figure 3 for the three-center HBr elimination, Figure 4 for the C−Br bond scission, and Figure 5 for the three-center H_2 elimination in vinyl bromide. For the sake of clarity, results are shown only for E = 5.23, 6.23, 6.98, and 7.67 eV. The plots of k versus q_C show interesting energy-dependent features, particularly for the two three-center elimination reactions. In the case of the HBr elimination, the minimum in the k-versus-q_C curve is found at q_C = 2.7−2.9 Å for E in the range 5.73−6.48 eV and at q_C = 2.3−2.4 Å for E in the range 6.73−7.67

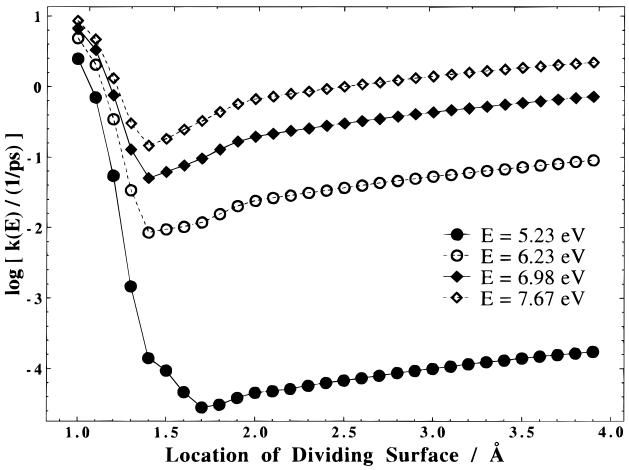

Figure 5. EMS-TST results for k_{HH}, the microcanonical rate constant for three-center H_2 elimination in vinyl bromide, as a function of transition-state dividing surface location, q_C. Results are shown for E = 5.23, 6.23, 6.98, and 7.67 eV. Lines connecting data points are for visual clarity only.

TABLE 3: Comparison of EMS-TST and Trajectory Values of the Rate Constant for Three-Center HBr Elimination in Vinyl Bromide[a] (Errors in the EMS-TST Results Are 95% Confidence Limits)

E/eV[b]	$k_{EMS-TST}$/ps^{-1}	$k_{trajectory}$/ps^{-1}
5.23	0.172 ± 0.013	0.117
5.73	0.574 ± 0.094	0.288
6.23	1.265 ± 0.133	0.465
6.48	1.653 ± 0.180	0.574
6.73	2.219 ± 0.291	0.739
6.98	2.613 ± 0.299	0.818
7.23	2.800 ± 0.153	0.925
7.67	3.274 ± 0.194	0.939

[a] Trajectory values obtained from ref 32, as described in the text. [b] For the EMS-TST calculations only; total energy for the trajectory calculations is 0.14 eV smaller.

TABLE 4: Comparison of EMS-TST and Trajectory Values of the Rate Constant for C−Br Bond Scission in Vinyl Bromide[a] (Errors in the EMS-TST Results Are 95% Confidence Limits)

E/eV[b]	$k_{EMS-TST}$/ps^{-1}	$k_{trajectory}$/ps^{-1}
5.23	0.00692 ± 0.00066	0.00945
5.73	0.0241 ± 0.0029	0.0355
6.23	0.0591 ± 0.0079	0.0397
6.48	0.0878 ± 0.0088	0.0779
6.73	0.123 ± 0.009	0.0880
6.98	0.157 ± 0.017	0.0819
7.23	0.198 ± 0.010	0.100
7.67	0.285 ± 0.027	0.0971

[a] Trajectory values obtained from ref 32, as described in the text. [b] For the EMS-TST calculations only; total energy for the trajectory calculations is 0.14 eV smaller.

eV. The presence of two minima in the graph is evident at all energies above and including 6.23 eV, with the inner one becoming more important as E increases. For the C−Br bond scission, the minimum in the k-versus-q_C curve lies at q_C = 4.6 Å for E = 5.23 eV and in the range 3.8 Å ≤ q_C ≤ 4.2 Å for all other energies, moving inward slowly as E increases. The shape of the curve indicates, however, that the values of k are nearly constant for a relatively large range of q_C values near the minimum. In the case of the H_2 elimination, the minimum in the k-versus-q_C curve lies at q_C = 1.7 Å for the two lowest energies and at q_C = 1.4 Å for all the remaining energies.

Tables 3 and 4 and Figures 6 and 7 show comparisons between the EMS-TST and trajectory values of $k(E)$ as a function of energy for the HBr elimination and C−Br bond scission, respectively. For the HBr elimination, $k_{EMS-TST}$ is larger than $k_{trajectory}$ at all of the energies considered, a result that is consistent with the conclusion that the HBr elimination is governed by statistical dynamics.[26−29] For the C−Br bond scission, $k_{EMS-TST}$ and $k_{trajectory}$ are approximately equal at E = 6.48 eV and below, and $k_{EMS-TST}$ is noticeably larger than $k_{trajectory}$ at E = 7.67 eV and above. At the two lowest energies, $k_{trajectory}$ is actually slightly larger than $k_{EMS-TST}$, but the difference is less than our estimate of the statistical error in the trajectory calculations at these energies. Thus, the C−Br bond scission may also be governed by statistical dynamics, particularly at higher energies. It is interesting that the EMS-TST calculations reproduce the surprising result from the trajectory study[32] that the rate constants for the HBr elimination are an order of magnitude larger than those for the C−Br bond scission. This is demonstrated by Table 5, which compares the EMS-TST and trajectory values of the ratio k_{HBr}/k_{C-Br} across the energy range. The EMS-TST values of this ratio are larger than the trajectory results at all energies, but agree to within at least a factor of 3 and often to better than a factor of 2. The fact that the trajectory calculations showed the rate constants for HBr elimination to be larger than those for C−Br bond scission is remarkable in that the energy threshold for the former reaction is 0.34 eV higher than that for the latter. This result was one piece of evidence leading to our earlier conjecture[32] that the

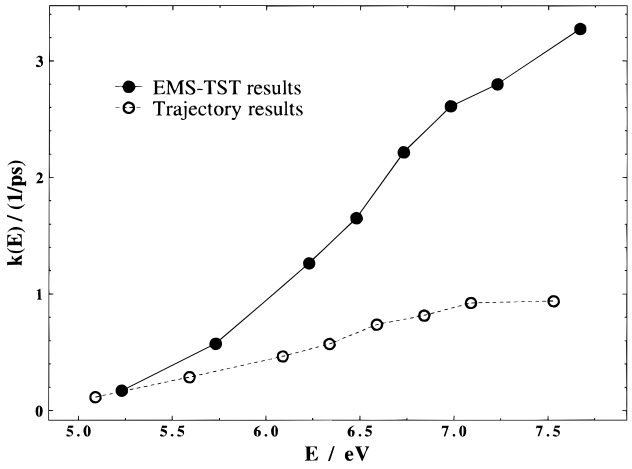

Figure 6. Comparison of EMS-TST and trajectory values of the rate constant for three-center HBr elimination in vinyl bromide, as a function of the total energy, E. Lines connecting data points are for visual clarity only.

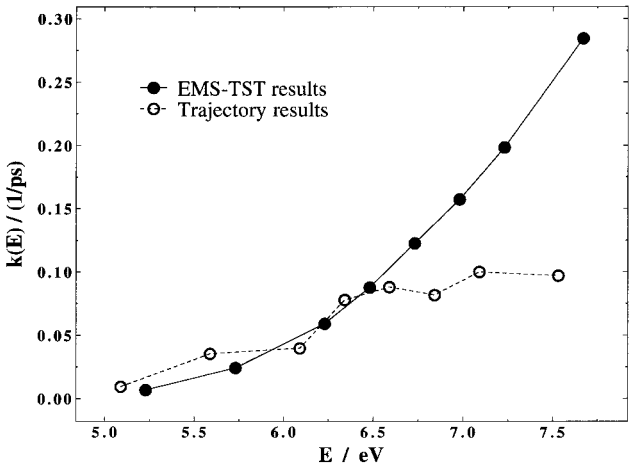

Figure 7. Comparison of EMS-TST and trajectory values of the rate constant for C−Br bond scission in vinyl bromide, as a function of the total energy, E. Lines connecting data points are for visual clarity only.

TABLE 5: Comparison of EMS-TST and Trajectory Values of k_{HBr}/k_{C-Br}, the Ratio of Rate Constants for Three-Center HBr Elimination and C−Br Bond Scission in Vinyl Bromide[a]

E/eV[b]	EMS-TST value	trajectory value
5.23	24.8	12.3
5.73	23.8	8.1
6.23	21.4	11.7
6.48	18.8	7.4
6.73	18.1	8.4
6.98	16.6	10.0
7.23	14.1	9.2
7.67	11.5	9.7

[a] Trajectory values obtained from ref 32. [b] For the EMS-TST calculations only; total energy for the trajectory calculations is 0.14 eV smaller.

TABLE 6: Comparison of EMS-TST and Trajectory Values of the Rate Constant for Three-Center H_2 Elimination in Vinyl Bromide[a] (Errors in the EMS-TST Results Are 95% Confidence Limits)

E/eV[b]	$k_{EMS-TST}$/ps^{-1}	$k_{trajectory}$/ps^{-1}
5.23	$(2.84 \pm 0.63) \times 10^{-5}$	*c*
5.73	0.00120 ± 0.00019	0.00559
6.23	0.00856 ± 0.00097	0.0183
6.48	0.0165 ± 0.00097	0.0505
6.73	0.0305 ± 0.0009	0.161
6.98	0.0506 ± 0.0050	0.259
7.23	0.0761 ± 0.0100	0.420
7.67	0.146 ± 0.014	1.015

[a] Trajectory values obtained from ref 32, as described in the text. [b] For the EMS-TST calculations only; total energy for the trajectory calculations is 0.14 eV smaller. [c] Below the detection limit of the trajectory calculations at this energy.

dynamics of vinyl bromide unimolecular dissociation are nonstatistical. Since the EMS-TST calculations reproduce the result, however, it would appear instead that the relatively low rate of C−Br bond scission arises from the topology of the potential surface rather than from nonstatistical dynamical effects. While this conclusion is strictly true only for our model vinyl bromide potential energy surface, we note with interest the results of recent experiments involving photolysis of bromoacetone,[42] which have shown that the C−Br bond scission is very slow relative to C−C bond scission even though the barrier to C−Br bond scission is much lower.

Table 6 and Figure 8 show comparisons between the EMS-TST and trajectory values of $k(E)$ as a function of energy for the H_2 elimination. The most striking feature of these results is that the values of $k_{trajectory}$ are larger than the $k_{EMS-TST}$ values throughout the energy range, by a factor of 2−4 at lower energies and a factor of 5−7 at higher energies. This necessarily means that nonstatistical dynamics govern this reaction,[26−29] which is a surprising result in view of the apparent statistical behavior of the HBr elimination and C−Br bond scission reactions. An examination of Figure 5 shows that at q_C values further out along the reaction coordinate, $k(E)$ at each energy increases from its minimum value to values larger than the trajectory result. Thus, the nonstatistical results arise because of the minimum in the k-versus-q_C plot at small values of q_C. Since there is no potential well or barrier to the back reaction along the minimum energy pathway for the three-center H_2 elimination on the potential energy surface used in the calculations,[32] it was not immediately apparent why the minimum in the plot should occur, so we devoted some effort to uncovering the origin of this feature.

Figure 9 shows how the minimum value of the potential energy attained at each transition-state dividing surface during the Markov walk varies with the location of the dividing surface,

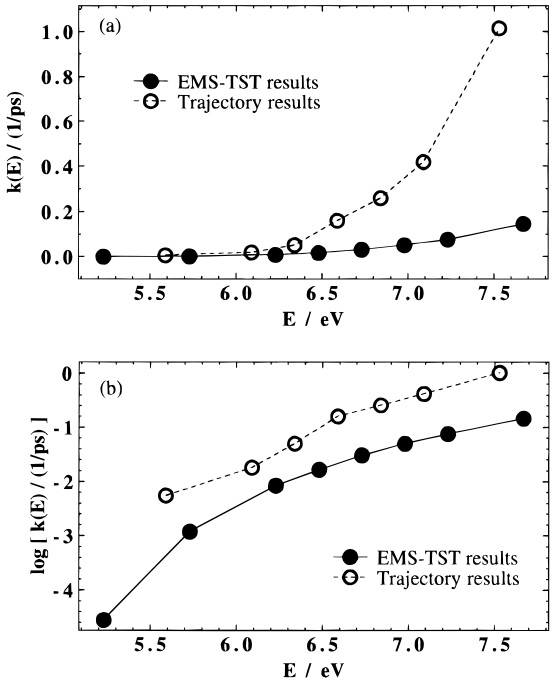

Figure 8. Comparison of EMS-TST and trajectory values of (a) the rate constant and (b) the base-10 logarithm of the rate constant for three-center H_2 elimination in vinyl bromide, as a function of the total energy, E. Lines connecting data points are for visual clarity only.

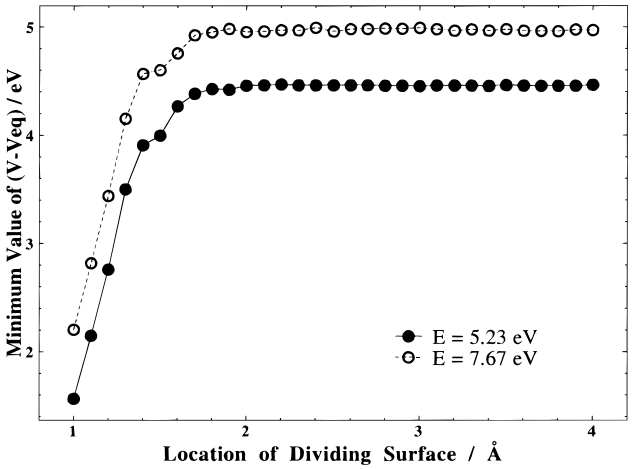

Figure 9. Minimum value of the potential energy V at each transition-state dividing surface for the three-center H_2 elimination, obtained by Markov walks at $E = 5.23$ and 7.67 eV. Ordinate values are plotted with respect to V_{eq}, the global minimum on the vinyl bromide potential energy surface. The curve for $E = 7.67$ eV has been displaced upward by 0.5 eV for visual clarity; lines connecting data points are also for visual clarity only.

q_C, for the H_2 elimination. For values of q_C greater than about 2 Å, the minimum potential energy is constant at 4.44 eV, which is equal to the barrier height for the reaction.[32] Thus, for q_C greater than about 2 Å, the interactions between the H_2 and C═CHBr fragments have disappeared and the system has reached product configuration space. In view of this, it is reasonable that any bottleneck to reaction should lie along the reaction coordinate at q_C less than 2 Å, where interactions between the separating fragments are still significant. An examination of the vinyl bromide structures associated with the minimum potential energy values from Figure 9 reveals that all of the structures for q_C less than 2 Å have the departing H_2 fragment aligned such that the H−H bond is perpendicular to the reaction coordinate, as shown in Figure 10. This suggested to us that the bottleneck to reaction that produces the minimum

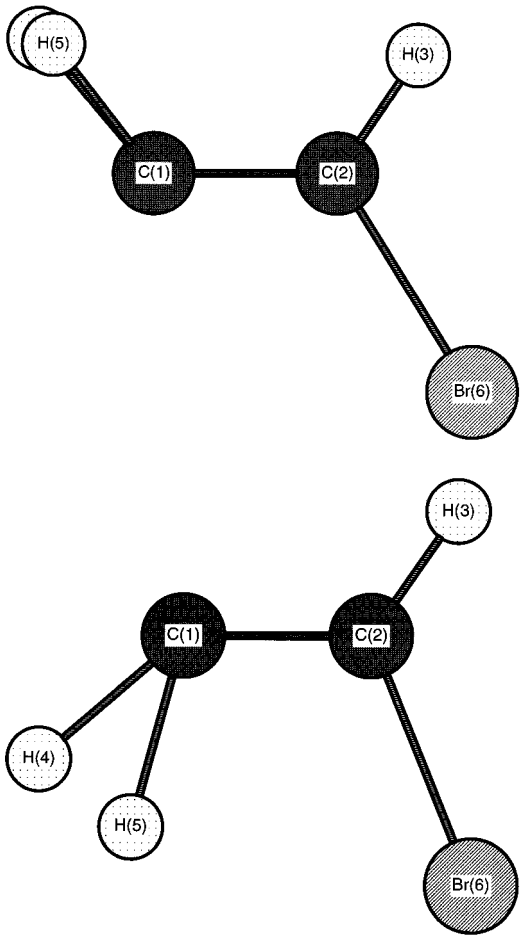

Figure 10. Minimum energy structures obtained by a Markov walk at $E = 5.23$ eV, at (a) $q_C = 1.3$ Å and (b) $q_C = 1.4$ Å along the reaction coordinate for three-center H_2 elimination. In each case, the C−C−Br plane coincides with the plane of the paper. In part a (top) the H^4-H^5 bond is nearly perpendicular to this plane, while in part b (bottom) the bond lies essentially in the plane. These represent extremes for the orientation of the CH_2 moiety in the minimum energy structures for $q_C < 2$ Å throughout the energy range. In each case, the figure shows that the H^4-H^5 bond is nearly perpendicular to the H_2 elimination reaction coordinate.

in the *k*-versus-q_C curves for the H_2 elimination may arise from hindering of the departing H_2 fragment's rotation in the C−H−H plane.

To test this hypothesis, we examined how the potential energy of the system varies with ϕ, the angle between the H−H bond and the reaction coordinate, at each of the transition-state dividing surfaces having $q_C < 2$ Å. To do this at a given dividing surface, we started from the coordinates of the minimum energy structure for that surface, rotated the H_2 fragment by small increments in the C−H−H plane while holding the coordinates of all the other atoms fixed, and calculated the potential energy of the system as a function of the rotation angle ϕ. By our definition, $\phi = 0°$ when the H−H bond lies along the reaction coordinate, and $\phi = \pm 90°$ when the H−H bond is perpendicular to the reaction coordinate. The results are shown as a surface plot in Figure 1l. The plot shows that the potential energy is symmetrical around $\phi = 0°$, as it ought to be when the two H atoms have identical masses, and that the potential energy is much larger for values of ϕ near 0° than for values of ϕ near ±90°. This confirms the presence of a configuration-space bottleneck to reaction that produces the minima in the *k*-versus-q_C curves for the H_2 elimination. We note that the sharp increase in potential energy at small ϕ as q_C goes from 1.3 to 1.4 Å gives rise to the minimum at $q_C = 1.4$ Å in the *k*-versus-q_C graphs at higher energies. Similarly, the drop in potential energy as q_C goes from 1.7 to 1.8 Å correlates with the minimum at $q_C = 1.7$ Å in the *k*-versus-q_C curves at low energies. It is likely that the double minima in the *k*-versus-q_C curves for the HBr elimination also arise because of a similar barrier to rotation of the departing HBr fragment.

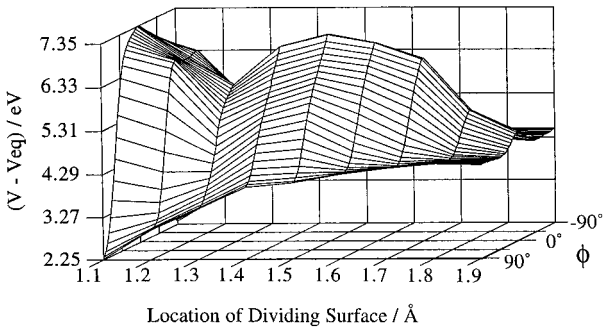

Figure 11. Variation of the potential energy V as a function of ϕ, the H_2-fragment rotation angle defined in the text, and q_C, the location of the transition-state dividing surface along the reaction coordinate for H_2 elimination. The potential energy values are given with respect to V_{eq}, the global minimum on the vinyl bromide potential energy surface. The spacing between grid lines in the ϕ direction is 4°.

TABLE 7: Vibrational Modes of Vinyl Bromide (Superscripts on Atomic Symbols Refer to the Atom Numbers Defined in Table 1)

mode designation	description of mode	frequency[a]/cm^{-1}
ν_1	C−C−Br bend	345
ν_2	CHBr wag	576
ν_3	C−Br stretch	623
ν_4	CH_2 wag	889
ν_5	CH_2−CHBr torsion	963
ν_6	C−C−H^5 bend	1004
ν_7	C−C−H^3 bend	1214
ν_8	H−C−H bend	1377
ν_9	C═C stretch	1606
ν_{10}	CH_2 symm. stretch	3004
ν_{11}	C−H^3 stretch	3086
ν_{12}	C−H_2 asymm. stretch	3121

[a] From normal-mode analysis on the vinyl bromide potential energy surface used here and in ref 32.

Given the existence of this bottleneck to H_2 elimination on the potential energy surface, the fact that $k_{trajectory} > k_{EMS-TST}$ means that the trajectory calculations do not reflect the presence of the bottleneck to the same extent that the EMS-TST calculations do. It seemed to us that this effect must arise because coupling of the departing H_2 fragment to the vibrational modes of the C═CHBr fragment breaks down as the trajectory proceeds. Since the basic assumption of EMS-TST and all other statistical reaction rate theories is that the internal energy of the system is globally randomized during the course of the reaction at a rate that is fast compared to the reaction rate, such a breakdown in coupling during the trajectories could trap energy in excess of the amount predicted by EMS-TST in the dissociation coordinate. This would lead to the result that $k_{trajectory} > k_{EMS-TST}$. To see whether this explanation is correct, we examined the IVR rates and pathways in vinyl bromide[33] using the projection method.[35] This technique extracts information about IVR in a molecule by analyzing the envelope functions of the temporal variations of a diagonal kinetic energy matrix for the molecular vibrational modes. Table 7 lists the 12 vibrational modes of vinyl bromide, for use as a reference in the discussion that follows. Our projection study first looked at IVR in vinyl bromide for configurations near the equilibrium configuration. The results showed that for each of the 12 vibrational modes excited with 3.0 eV of energy in excess of

zero-point energy, the total IVR rate out of the mode is a factor of 3−12 larger than the trajectory-computed total decomposition rate of vinyl bromide having an excitation energy of 6.44 eV. However, not all of the mode-to-mode IVR rates are large compared to the reaction rate, so that IVR is not *globally* fast on the time scale of the decomposition reaction. Taken together, these two results mean that over the energy range studied here it is possible for the system to exhibit statistical behavior, but such behavior is not guaranteed.[26−28,31,33]

In addition to the above, we also investigated IVR rates in vinyl bromide for configurations far from equilibrium, lying along the reaction coordinates for the H_2 and HBr elimination reactions. To do this, we used as the initial configurations for the projection method the minimum energy structures found by the EMS-TST Markov walk at various transition-state dividing surfaces near the optimum surface, at $E = 7.67$ eV. The kinetic energy, K, for the initial structure was randomly distributed over the vibrational modes, as described in ref 33. Figure 7 of ref 33 shows the temporal variation of the mode kinetic energies for a vinyl bromide trajectory whose initial configuration was the minimum energy structure at $q_C = 1.0$ Å along the H_2 elimination reaction coordinate. This particular trajectory sampled phase space in the transition-state region for about 50 time units (tu; 1 tu = 0.01018 ps), after which it re-entered reactant phase space. An examination of the various traces shows that the CH_2 wag (ν_4), the C−C−H[5] bend (ν_6), the H−C−H bend (ν_8), the C−H stretch (ν_{10}, ν_{11}, ν_{12}), the C=C stretch (ν_9), and the CH_2−CHBr torsion (ν_5) modes all gain relatively large amounts of kinetic energy in the first few time units of the trajectory, while the C−C−H[3] bend (ν_7) and the Br modes (ν_1, ν_2, ν_3) gain small amounts of kinetic energy. The group of modes that gain energy include all five of the modes (ν_4, ν_6, ν_8, ν_{10}, ν_{12}) that contribute to motion along the reaction coordinate. At roughly $t = 20$ tu, the energies in the CH_2 wag (ν_4) and the C−H[3] stretch (ν_{11}) decrease to nearly zero. This energy is transferred primarily to ν_5, ν_6, ν_8, ν_9, and ν_{10}, all of which are modes belonging to the group that gained energy early in the trajectory. By $t = 40$ tu, four of the five modes contributing to motion along the reaction coordinate (all but ν_4) are still highly excited. Throughout the whole time period, the C−C−H[3] bend (ν_7) and the Br modes (ν_1, ν_2, ν_3) remain relatively uninvolved in the overall IVR dynamics, and it is clear that the IVR process as a whole is not globally rapid. These results support our contention that the mode-to-mode coupling breaks down to some extent for configurations along the reaction coordinate for H_2 elimination, in such a way that energy can be trapped in the dissociation coordinate.

In contrast to this situation, Figure 8 of ref 33 shows the temporal variation of the mode kinetic energies for a vinyl bromide trajectory whose initial configuration was the minimum energy structure at $q_C = 2.3$ Å along the HBr elimination reaction coordinate. This trajectory sampled phase space along the reaction coordinate for about 25 tu (0.255 ps), after which dissociation to HBr occurred. The temporal variation of the mode kinetic energies shown in this figure clearly demonstrates (1) that all of the vibrational modes except the C−C−Br bend (ν_1) participate fully in the IVR dynamics throughout the time period before reaction and (2) that the internal energy is essentially globally randomized at a rate that is fast compared to the unimolecular decomposition rate. These results indicate that the HBr elimination ought to be well-described by statistical reaction rate theory, as the EMS-TST calculations reported here for that reaction have demonstrated. Thus we are led to the interesting result that in vinyl bromide some of the unimolecular decomposition reactions (e.g., the three-center HBr elimination) are governed by statistical dynamics, while others (e.g., the three-center H_2 elimination) involve nonstatistical dynamics.

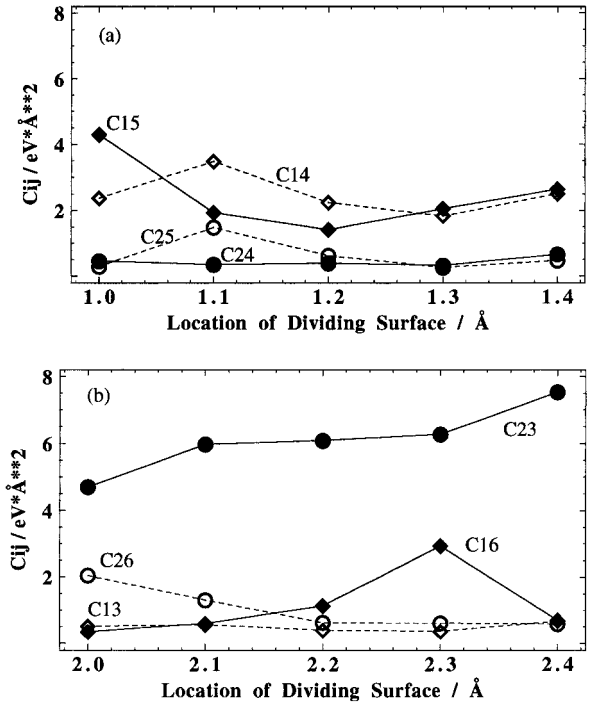

Figure 12. (a) Atom−atom coupling constants C_{ij} between atoms of the carbon chain ($i = 1, 2$) and atoms of the H_2 fragment ($j = 4, 5$), as a function of dividing surface location q_C along the reaction coordinate for three-center H_2 elimination. (b) Coupling constants C_{ij} between atoms of the carbon chain ($i = 1, 2$) and atoms of the HBr fragment ($j = 3, 6$), as a function of dividing surface location q_C along the reaction coordinate for three-center HBr elimination. Atom numbers (i and j) are defined in Table 1. Lines connecting data points are for visual clarity only.

An alternative method for comparing the relative magnitudes of the mode-to-mode coupling in the H_2 and HBr elimination reactions is provided by the calculation of atom−atom coupling constants, C_{ij}, defined by[29]

$$C_{ij} \equiv \frac{1}{9}\sqrt{\sum_{\alpha=1}^{3}\sum_{\beta=1}^{3}\left[\frac{\partial^2 V}{\partial q_{\alpha i}\,\partial q_{\beta j}}\right]^2} \qquad (12)$$

in which α and β run over the three Cartesian coordinates [$(x,y,z) \equiv (q_1,q_2,q_3)$] of atoms i and j, respectively. The C_{ij} are invariant to translations of or rotations around the molecule's center of mass and provide a direct measure of the extent of potential coupling in the molecule.[29] We calculated values of C_{ij} as a function of q_C, using the minimum energy structures at various dividing surfaces in the transition-state regions for the H_2 and HBr eliminations. These structures were found by Markov walks at $E = 7.67$ eV. Part a of Figure 12 shows coupling constants C_{ij} between the atoms of the carbon chain ($i = 1, 2$) and the atoms of the H_2 fragment ($j = 4, 5$) for structures found along the H_2 elimination reaction coordinate, while part (b) shows C_{ij} between the carbon-chain atoms and the atoms of the HBr fragment ($j = 3, 6$) for structures found along the HBr elimination reaction coordinate. Clearly, the largest of the coupling constants is C_{23}, which measures the coupling between the H atom of the HBr fragment and the carbon atom to which it is directly bonded. C_{23} is larger than C_{14} and C_{15}, the analogous C−H interactions for the H_2 elimination. In addition, C_{23} increases as the system moves out along the HBr reaction coordinate, while C_{14} and C_{15} decrease as the system moves out along the H_2 reaction coordinate. Another interesting feature

of Figure 12 is that C_{16}, which measures the next-nearest-neighbor interaction between the Br atom and the carbon to which it is not directly bonded, becomes increasingly important as the system moves out along the HBr reaction coordinate. In contrast, the corresponding next-nearest-neighbor couplings for the H_2 elimination, C_{24} and C_{25}, are small and, for the most part, either constant or decreasing as the system moves out along the H_2 reaction coordinate. All of these results are consistent with the picture of vinyl bromide IVR drawn by the projection study described above and thus support the general conclusion we have made about the differing natures of the dynamics governing the three-center H_2 and HBr elimination reactions on our model potential surface for vinyl bromide.

It is important to note that all of the above conclusions apply to a model system whose potential energy surface is the analytic surface described in ref 32. This potential has been fitted to a data base comprising transition-state energies computed by *ab initio* methods at the MP4 and QCISD(T) levels of theory using 6-311G(d,p) and 6-311+G(2df,p) basis sets, experimental geometries, and vibrational frequencies for all reactants and products, and measured heats of reaction for all energetically open reaction channels. Analysis of the surface[32] shows that, in many respects, the result is a reasonably accurate representation of the experimental vinyl bromide system. Equilibrium bond distances are predicted to within 0.082 Å or better. The average deviation of the fundamental vibrational frequencies predicted by the analytic surface and those obtained from either experiment or *ab initio* theory is 10.2 cm^{-1} for $H_2C{=}CHBr$, 12.0 cm^{-1} for acetylene, 25.3 cm^{-1} for $H_2C{=}CDBr$, 46.3 cm^{-1} for $D_2C{=}CDBr$, 78 cm^{-1} for $D_2C{=}CHBr$, and 81.3 cm^{-1} for $H_2C{=}CH$. The average absolute error in the predicted potential barriers for five decomposition channels of vinyl bromide and for the vinylidene → acetylene isomerization is 0.125 eV. The average absolute error in the predicted heats of reaction for these channels is 0.083 eV.

Although the above properties of vinyl bromide are represented with good accuracy by the analytic potential, properties of the transition states other than their energies are not so well-described. For example, the C−H stretching frequencies obtained from the analytic surface at the transition state for four-center HBr elimination are in very poor agreement with the *ab initio* calculations. The same is true for one of the C−H stretches and for the imaginary frequency along the reaction coordinate for the four-center H_2 elimination. The geometries in the transition states are also not well-described. These defects arise primarily because the surface properties in the transition-state regions are strongly dependent upon the switching functions employed to connect the various reaction channels. Each of these functions contains only a single adjustable parameter, which has been used to fit the computed or measured potential barriers. The analytic potential therefore does not contain sufficient flexibility to permit fitting the transition-state structures and frequencies. The strengths and weaknesses of the potential have been discussed in quantitative detail elsewhere.[32]

Since the potential surface employed in the vinyl bromide studies is known to be deficient in several respects, we cannot determine which of the effects leading to nonstatistical behavior actually represent the experimental vinyl bromide system and which might be artifacts of inaccuracies in our potential. Such a determination would require the formulation of a more accurate vinyl bromide potential. However, the present investigation does show that a system may exist for which IVR rates along some reaction channels are sufficiently rapid to produce statistical dynamics, whereas for other decomposition channels the IVR rates are slow enough to make the dynamics nonstatistical. It seems to us that such a situation is likely to be realized experimentally in large polyatomic systems with many vibrational modes and decomposition pathways, even if it does not occur experimentally in vinyl bromide but arises in the present work as an artifact of the potential surface.

IV. Summary

We have computed rate constants for three unimolecular decomposition reactions of vinyl bromide for several energies in the range 5.23−7.67 eV, using statistical variational efficient microcanonical sampling−transition-state theory (EMS-TST)[26] on our previously reported[32] global vinyl bromide potential energy surface. We have compared the EMS-TST results with those obtained from our classical trajectory study[32] on the same potential energy surface in order to assess the extent to which vinyl bromide unimolecular decomposition is governed by statistical dynamics.

For the three-center HBr elimination reaction, we find that $k_{EMS-TST}$ is greater than $k_{trajectory}$ by a factor of 1.5−3.5 over the energy range considered. For the C−Br bond scission, the EMS-TST and trajectory results at lower energies are equal within the statistical error in the trajectory calculations, while at higher energies $k_{EMS-TST}$ is greater than $k_{trajectory}$ by a factor of 1.4−2.9. The EMS-TST calculations also reproduce a surprising result from the trajectory study, that the rate constant for three-center HBr elimination is an order of magnitude greater than that for C−Br bond scission throughout the energy range, even though the barrier height for the latter reaction is 0.34 eV lower. These results imply that three-center HBr elimination and C−Br bond scission are governed by statistical dynamics.

On the other hand, for the three-center H_2 elimination reaction we find that $k_{trajectory}$ is greater than $k_{EMS-TST}$, by a factor of 2−4 at lower energies and a factor of 5−7 at higher energies. This result necessarily implies that the dynamics of the three-center H_2 elimination are nonstatistical. The nonstatistical behavior for this reaction is attributed to a breakdown in the coupling among vibrational modes as the H_2 fragment departs, which leaves energy in excess of the statistically predicted amount in the dissociation coordinate. A study of IVR rates and pathways in vinyl bromide[33] supports this conclusion. The IVR analysis also shows that such a breakdown in mode-to-mode coupling does not exist for the three-center HBr elimination and that nearly global randomization of the internal energy rapidly occurs as the system moves through the transition-state region for HBr elimination. Thus, the nature of IVR on our vinyl bromide potential surface is consistent with the present EMS-TST results showing that three-center HBr elimination is well-described by statistical reaction-rate theory, while three-center H_2 elimination is not.

Acknowledgment. We are pleased to acknowledge financial support from the National Science Foundation under Grant CHE-9211925. R.D.K. also gratefully acknowledges Gordon College for financial support during his sabbatical, the Gordon College Faculty Development Program for a travel grant, and Dr. Dan Sorescu and Dr. Ran Pan for stimulating and helpful discussions.

References and Notes

(1) Pechukas, P. *Ann. Rev. Phys. Chem.* **1981**, *32*, 159.
(2) Peslherbe, G. H.; Hase, W. L. *J. Chem. Phys.* **1994**, *101*, 8535.
(3) Klippenstein, S. J.; Koess, J. D. *J. Chem. Phys.* **1992**, *96*, 8164.
(4) Klippenstein, S. J.; Radivoyevitch, T. *J. Chem. Phys.* **1993**, ***99***, 3644.
(5) Hu, X.; Hase, W. L. *J. Chem. Phys.* **1991**, *95*, 8073; **1992**, *96*, 5558.

(6) Truong, T. N.; Truhlar, D. G. *J. Chem. Phys*. **1990**, *93*, 1761; **1992**, *97*, 8820.
(7) Melissas, V. S.; Truhlar, D. G. *J. Chem. Phys*. **1993**, *99*, 1013; **1993**, *99*, 3542.
(8) Gonzales-Lafont, A.; Truong, T. N.; Truhlar, D. G. *J. Chem. Phys.* **1991**, *95*, 8875.
(9) Park, J.; Bersohn, R.; Oref, I. *J. Chem. Phys.* **1990**, *93*, 5700.
(10) Yi, W.; Chattopadhyay, A.; Bersohn, R. *J. Chem. Phys*. **1991**, *94*, 4817.
(11) Holland, J. P.; Rosenfeld, R. N. *J. Chem. Phys*. **1988**, *89*, 7217.
(12) Light, J. C.; Lin, J. *J. Chem. Phys*. **1965**, *43*, 3209.
(13) Pechukas, P.; Light, J. C. *J. Chem. Phys.* **1965**, *42*, 3281.
(14) Viggiano, A. A.; Morris, R. A.; Paschkewitz, J. S.; Paulson, J. F. *J. Am. Chem. Soc*. **1992**, *114*, 10477.
(15) Graul, S. T.; Bowers, M. T. *J. Am. Chem. Soc*. **1991**, *113*, 9696.
(16) VanOrden, S. L.; Pope, R. M.; Brauman, S. W. *J. Am. Chem. Soc*. **1992**, *114*, 9706.
(17) Cho, Y. J.; Vande Linde, S. R.; Zhu, L.; Hase, W. L. *J. Chem. Phys*. **1992**, *96*, 8275.
(18) Hase, W. L.; Cho, Y. J. *J. Chem. Phys*. **1993**, *98*, 8626.
(19) Vande Linde, S. R.; Hase, W. L. *J. Phys. Chem*. **1990**, *94*, 6148; *J. Chem. Phys.* **1990**, *93*, 7962.
(20) Lyons, B. A.; Pfeifer, J.; Carpenter, B. K. *J. Am. Chem. Soc*. **1991**, *113*, 9006.
(21) Peterson, T. H.; Carpenter, B. K. *J. Am. Chem. Soc*. **1992**, *114*, 766.
(22) Carpenter, B. K. *Acc. Chem. Res.* **1992**, *25*, 520.
(23) Lyons, B. A.; Pfeifer, J.; Peterson, T. H.; Carpenter, B. K. *J. Am. Chem. Soc.* **1993**, *115*, 2427.
(24) Carpenter, B. K. *J. Am. Chem. Soc.* **1995**, *117*, 6336.
(25) Schranz, H. W.; Raff, L. M.; Thompson, D. L. *Chem. Phys. Lett*. **1990**, *171*, 68.
(26) Schranz, H. W.; Raff, L. M.; Thompson, D. L. *J. Chem. Phys.* **1991**, *94*, 4219.
(27) Schranz, H. W.; Raff, L. M.; Thompson, D. L. *Chem. Phys. Lett.* **1991**, *182*, 455.
(28) Schranz, H. W.; Raff, L. M.; Thompson, D. L. *J. Chem. Phys*. **1991**, *95*, 106.
(29) Sewell, T. D.; Schranz, H. W.; Thompson, D. L.; Raff, L. M. *J. Chem. Phys.* **1991**, *95*, 8089.
(30) Alimi, R.; Apkarian, V. A.; Gerber, R. B. *J. Chem. Phys.* **1993**, *98*, 331.
(31) Raff, L. M. *J. Chem. Phys.* **1989**, *90*, 6313.
(32) Abrash, S. A.; Zehner, R. W.; Mains, G. J.; Raff, L. M. *J. Phys. Chem*. **1995**, *99*, 2959.
(33) Pan, R.; Raff, L. M. *J. Phys. Chem.* **1996**, *100*, 8085.
(34) Sorescu, D. C.; Thompson, D. L.; Raff, L. M. *J. Chem. Phys*. **1994**, *101*, 3729.
(35) Raff, L. M. *J. Chem. Phys*. **1988**, *89*, 5680.
(36) Doll, J. D. *J. Chem. Phys.* **1980**, *73*, 2760; **1981**, *74*, 1074.
(37) Metropolis, N.; Rosenbluth, A. W.; Rosenbluth, M. N.; Teller, A. H.; Teller, E. *J. Chem. Phys.* **1953**, *21*, 1087.
(38) Brady, J. W.; Doll, J. D.; Thompson, D. L. *J. Chem. Phys.* **1981**, *74*, 1026; Adams, J. E. *J. Chem. Phys.* **1983**, *78*, 1295. Viswanathan, R.; Thompson, D. L.; Raff, L. M. *J. Chem. Phys.* **1984**, *80*, 4230. Viswanathan, R.; Thompson, D. L.; Raff, L. M. *J. Chem. Phys.* **1984**, *81*, 3118.
(39) Schranz, H. W.; Nordholm, S.; Nyman, G. *J. Chem. Phys.* **1991**, *94*, 1487.
(40) Severin, E. S.; Freasier, B. C.; Hamer, N. D.; Jolly, D. L.; Nordholm, S. *Chem. Phys. Lett.* **1978**, *57*, 117; Severin, E. S. Thesis BSc. Honors, University of New South Wales, R. M. C. Duntroon, 1977.
(41) Sorescu, D. C.; Thompson, D. L.; Raff, L. M. *J. Chem. Phys*. **1995**, *103*, 5387.
(42) Kash, P. W.; Waschewsky, G. C. G.; Morss, R. E.; Butler, L. J.; Francl, M. M. *J. Chem. Phys.* **1994**, *100*, 3463.